

RESEARCH

Open Access



Association of pericoronary inflammation with atherosclerotic plaque progression in diabetic patients with improved modifiable cardiovascular risk factors: a longitudinal CCTA cohort study

Tianhao Zhang^{1†}, Hongkai Zhang^{2†}, Xuelian Gao⁴, Pingan Peng¹, Tianlong Chen³, Xiaoming Zhang¹, Jingyao Yang¹, Yang Zheng¹, Yulu Peng¹, Xiaonan Ma¹, Dongmei Shi¹, Zhijian Wang¹, Lei Xu², Yujie Zhou^{1,3} and Yu Du^{1*}

Abstract

Background Pericoronary adipose tissue (PCAT) attenuation, as assessed by coronary computed tomography angiography (CCTA), has been identified as a marker of pericoronary inflammation and a predictor of future adverse atherosclerotic events. However, the impact of changes in PCAT attenuation, as evaluated by consecutive CCTAs, on plaque progression in high-risk atherosclerotic patients with improved modifiable cardiovascular risk factors (mCRFs) remains unclear.

Methods Consecutive patients with type 2 diabetes mellitus (T2DM) who had improved mCRFs and underwent serial, clinically indicated CCTA examinations (time interval ≥ 12 months) at our center between July 2019 and July 2022 were screened. Eligible participants had at least one study plaque, defined as a plaque without significant anatomic stenosis, located in one of the major coronary arteries, which had not been intervened upon or caused adverse events between serial CCTA scans. Percent atheroma volume (PAV) and PCAT attenuation were measured for each study plaque at baseline and follow-up using CCTA plaque analysis software. Changes in PAV (δ PAV = follow-up PAV – baseline PAV) were compared based on changes in PCAT attenuation [δ PCAT attenuation] (> 0 or ≤ 0). Multivariate linear regression models were used to evaluate the relationship between δ PCAT attenuation and δ PAV.

Results A total of 98 T2DM patients (mean age: 59.9 years; 75.3% men; 152 plaques) had mCRFs that reached therapeutic targets at follow-up CCTA. However, overall PAV progressed from baseline in all patients [(41.68 \pm 12.47)% vs. (43.71 \pm 12.24)%, $p = 0.035$], accompanied by an increase in coronary inflammation (i.e., PCAT attenuation) during a median follow-up of 13.5 months (interquartile range [IQR]: 12.2, 17.5 months). Compared to patients with δ PCAT

[†]Tianhao Zhang and Hongkai Zhang contributed equally to this work.

*Correspondence:

Yu Du
duyupla0604@outlook.com

Full list of author information is available at the end of the article



attenuation ≤ 0 , those with δ PCAT attenuation > 0 had a significantly greater increase in overall PAV from baseline [(4.09 \pm 12.09)% vs. (-0.82 \pm 10.74)%, $p=0.011$], calcified PAV [1.57% (IQR: 0.13%, 3.84%) vs. 0.38% (IQR: -0.26%, 2.58%), $p=0.008$], and a numerical but non-significant increase in non-calcified PAV [(1.29 \pm 11.75)% vs. (-1.87 \pm 10.47)%, $p=0.089$]. Multivariate linear regression models demonstrated that increased PCAT attenuation was significantly associated with the progression of overall PAV ($\beta=0.339$, 95% CI: 0.129–0.549), non-calcified PAV ($\beta=0.237$, 95% CI: 0.019–0.455), and calcified PAV ($\beta=0.109$, 95% CI: 0.019–0.200), independent of age, sex, cardiovascular risk factors, medications, and baseline PCAT attenuation and PAV (all $p < 0.05$). The effect of elevated PCAT attenuation on overall plaque progression was consistent across subgroups (all p for interaction > 0.05).

Conclusion In this longitudinal CCTA cohort of T2DM patients with improved mCRFs, increased pericoronary inflammation was associated with the progression of atherosclerotic plaque, particularly non-calcified plaque.

Keywords Pericoronary adipose tissue, Atherosclerotic plaque, Coronary computed tomography angiography, Type 2 diabetes mellitus

Introduction

Coronary artery disease (CAD) remains the leading cause of mortality and morbidity worldwide. Current strategies to prevent the progression of atherosclerosis emphasize lifestyle modifications and management of traditional risk factors [1, 2]. However, despite controlling modifiable cardiovascular risk factors (mCRFs), CAD patients continue to face a persistent risk of cardiovascular events, known as residual cardiovascular risk [3, 4]. Therefore, managing CAD requires addressing residual cardiovascular risk beyond achieving targets for mCRFs such as hypertension, type 2 diabetes mellitus (T2DM), and hypercholesterolemia.

Inflammation plays a key role in residual risk, contributing to the development, destabilization, and rupture of atherosclerotic plaques [5, 6]. A collaborative analysis of 31,245 atherosclerotic patients on statins demonstrated that systemic inflammation, measured by high-sensitivity C-reactive protein (hs-CRP), was a stronger predictor of future cardiovascular events than low-density lipoprotein cholesterol (LDL-C) [7]. Additionally, the Canakinumab Anti-inflammatory Thrombosis Outcomes Study trial showed that the interleukin-1 β inhibitor canakinumab significantly reduced adverse cardiovascular events in statin-treated CAD patients with hs-CRP ≥ 2 mg/L [8]. These findings highlighted the importance of evaluating residual inflammatory risk for risk stratification in statin-treated CAD patients [9]. However, the prognostic value of residual inflammatory risk has not been specifically examined in CAD patients with well-controlled traditional risk factors.

Pericoronary adipose tissue (PCAT) attenuation, measured using coronary computed tomography angiography (CCTA), has emerged as a more accurate biomarker of pericoronary inflammation compared to hs-CRP [10, 11]. Therefore, we constructed a T2DM cohort with inherently increased vessel-level inflammation and a higher risk of future cardiovascular events [12]. In this longitudinal cohort, where cardiovascular risk profiles improved

between consecutive CCTAs, we utilized advanced CCTA post-processing software to investigate the independent association between changes in PCAT attenuation and the progression of atherosclerotic plaques.

Method

Study design and patients

This retrospective study screened consecutive patients with T2DM presenting with chest pain who underwent at least two clinically indicated CCTA examinations at Beijing Anzhen Hospital, Capital Medical University, between July 2019 and July 2022. Eligible participants had at least one study plaque, defined as a plaque with $< 70\%$ diameter stenosis in a major coronary artery, which was neither intervened upon nor associated with plaque-related adverse events between serial CCTA scans. Major exclusion criteria included: (1) A time interval of < 12 months between baseline and the last CCTA scan; (2) Incomplete clinical or laboratory data; (3) Inadequate CCTA image quality for analysis; (4) Uncontrolled mCRFs at the last CCTA follow-up, including blood pressure (BP) $\geq 140/90$ mmHg, fasting plasma glucose (FPG) ≥ 8.0 mmol/L, LDL-C ≥ 1.8 mmol/L, or hs-CRP ≥ 2.0 mmol/L (Fig. 1). The study was conducted in accordance with the Declaration of Helsinki and approved by the Medical Ethics Committee of Beijing Anzhen Hospital, Capital Medical University. Informed consent was obtained from all participants.

Data collection and follow-up

Demographic information, mCRFs, medical histories, laboratory findings, CCTA scan parameters, and medication data for eligible patients were obtained from electronic medical records. To assess the management of mCRFs, the levels of BP, fasting plasma glucose, LDL-C, and hs-CRP were recorded at both baseline and the final CCTA scan. Follow-up was conducted through outpatient visits or telephone interviews to identify plaque-related adverse events, including cardiac death,

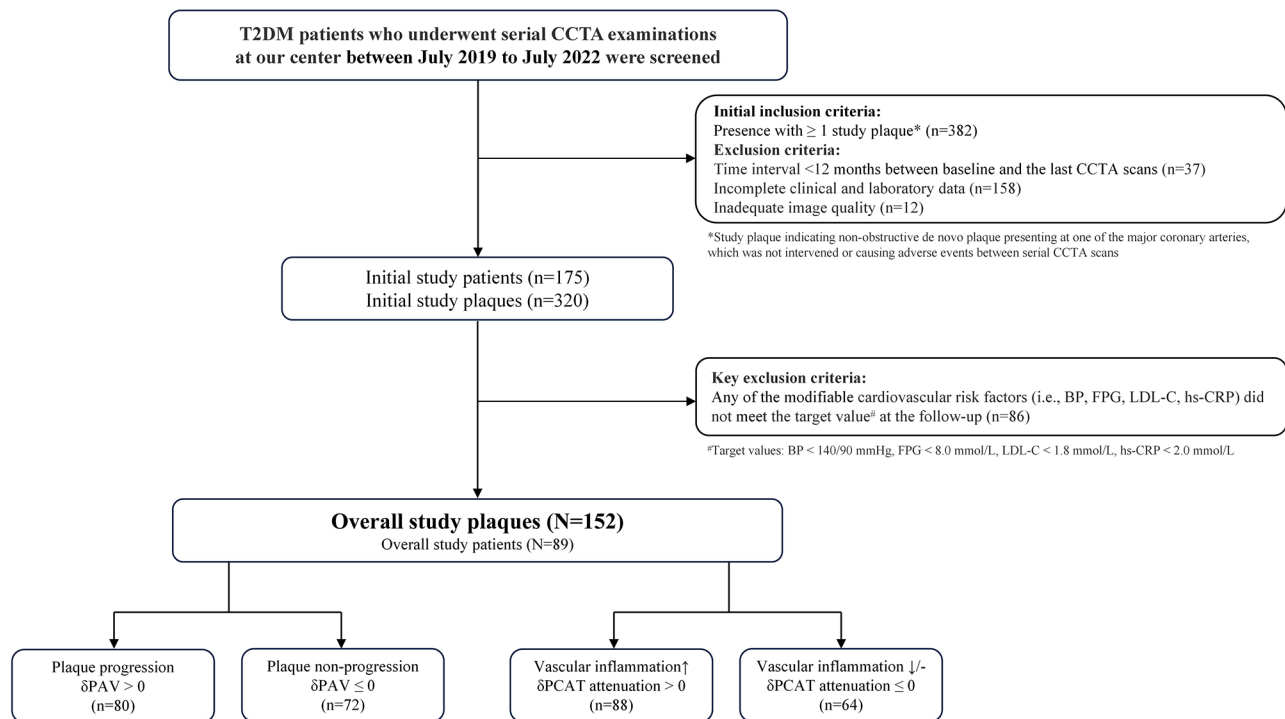


Fig. 1 Study flow-chart. Abbreviations: BP, blood pressure; CCTA, coronary computed tomographic angiography; FPG, fasting plasma glucose; hs-CRP, high-sensitivity C-reactive protein; LDL-C, low-density lipoprotein cholesterol; PAV, percent atheroma volume; PCAT: pericoronary adipose tissue; T2DM, type 2 diabetes mellitus

myocardial infarction, or revascularization occurring between serial CCTA scans.

CCTA image acquisition

Following the guidelines of the Society of Cardiovascular Computed Tomography [13], the CCTA acquisition parameters were consistent at baseline and follow-up for all study participants. Each patient received an injection of 40–60 mL of contrast media (Ultravist, Bayer; 370 mg iodine/mL) into the antecubital vein at a rate of 4–5 mL/s, followed by a 30mL saline flush. Image acquisition was performed using a 256-slice CT scanner (Revolution CT, GE Healthcare, USA). Additional scan parameters included a reconstructed slice thickness of 0.625 mm, a gantry rotation time of 0.28 s, and a tube voltage of 100 or 120 kV.

Plaque identification and quantitative analysis

Anonymous CCTA datasets were transferred to an offline workstation for quantitative plaque analysis using semiautomated software (Circle Cardiovascular Imaging, Canada, Version 5.13), with manual corrections applied as needed. Segments of major epicardial coronary arteries with a diameter ≥ 2 mm were evaluated based on a modified 17-segment model. The presence of plaque was defined as any tissue ≥ 1 mm³ within or adjacent to the lumen that could be distinguished from surrounding structures and identified in at least two consecutive planes. To assess changes in plaque

burden, non-obstructive de novo plaques located in major coronary arteries, which were not intervened upon or associated with adverse events between serial CCTA scans, were included in the analysis. Three-dimensional quantitative parameters included overall and compositional percent atheroma volume (PAV). PAV was calculated as plaque volume multiplied by 100% and divided by vessel volume. Plaque composition was categorized into groups using Hounsfield unit (HU) thresholds: calcified (≥ 350 HU), non-calcified (< 350 HU), and low-attenuation (< 30 HU) [14–16]. For longitudinal analysis of PAV changes, plaques were co-registered using consistent anatomical landmarks, such as the distance from the ostium or branch vessels.

Pericoronary inflammation analysis

PCAT on CCTA was defined as fat within a radial distance from the outer vessel wall equal to the diameter of the coronary vessel, with pixels in the range of -190 to -30 HU [10, 17]. PCAT attenuation values for the proximal segments of the major coronary arteries were semi-automatically quantified from CCTA images using post-processing software (Shukun Technology, Beijing) by adjusting the technical parameters. The analysis focused on the proximal 10–50 mm segment of the right coronary artery (RCA) and the proximal 40 mm segment of the left anterior descending artery (LAD) and left circumflex artery (LCX), measured from the bifurcation of the left main artery. Representative

cases showing dynamic changes in PCAT attenuation and coronary plaque burden are presented in Fig. 2.

All CCTA images were analyzed for plaque characteristics and pericoronary inflammation by independent level-III experts who were blinded to the sequence and clinical details of the baseline and follow-up CCTA scans. To assess inter- and intra-observer variability, a second level-III reader re-analyzed 8 randomly selected plaques and instances of pericoronary inflammation, while the original level-III reader repeated the analysis on 8 randomly selected plaques and instances of pericoronary inflammation 3 months after the initial evaluation.

Statistical analysis

Continuous variables were presented as mean \pm standard deviation or as medians with interquartile ranges (IQR),

depending on data distribution. Group comparisons were performed using paired or unpaired Student's t-test or the Mann–Whitney U-test, as appropriate. Categorical variables were reported as frequencies (percentages) and compared using the chi-square test or Fisher's exact test.

Plaque-level analyses were conducted by categorizing study plaques based on either plaque progression (changes in PAV [δ PAV] >0 vs. δ PAV ≤ 0) or inflammation progression (changes in PCAT attenuation [δ PCAT attenuation] >0 vs. δ PCAT attenuation ≤ 0) between baseline and follow-up CCTA scans. Correlations between δ PCAT attenuation and changes in overall or compositional PAV were assessed using Pearson or Spearman correlation analyses. To evaluate the association of δ PCAT attenuation with δ PAV, multivariate linear regression was performed, with δ PCAT attenuation as the independent variable and

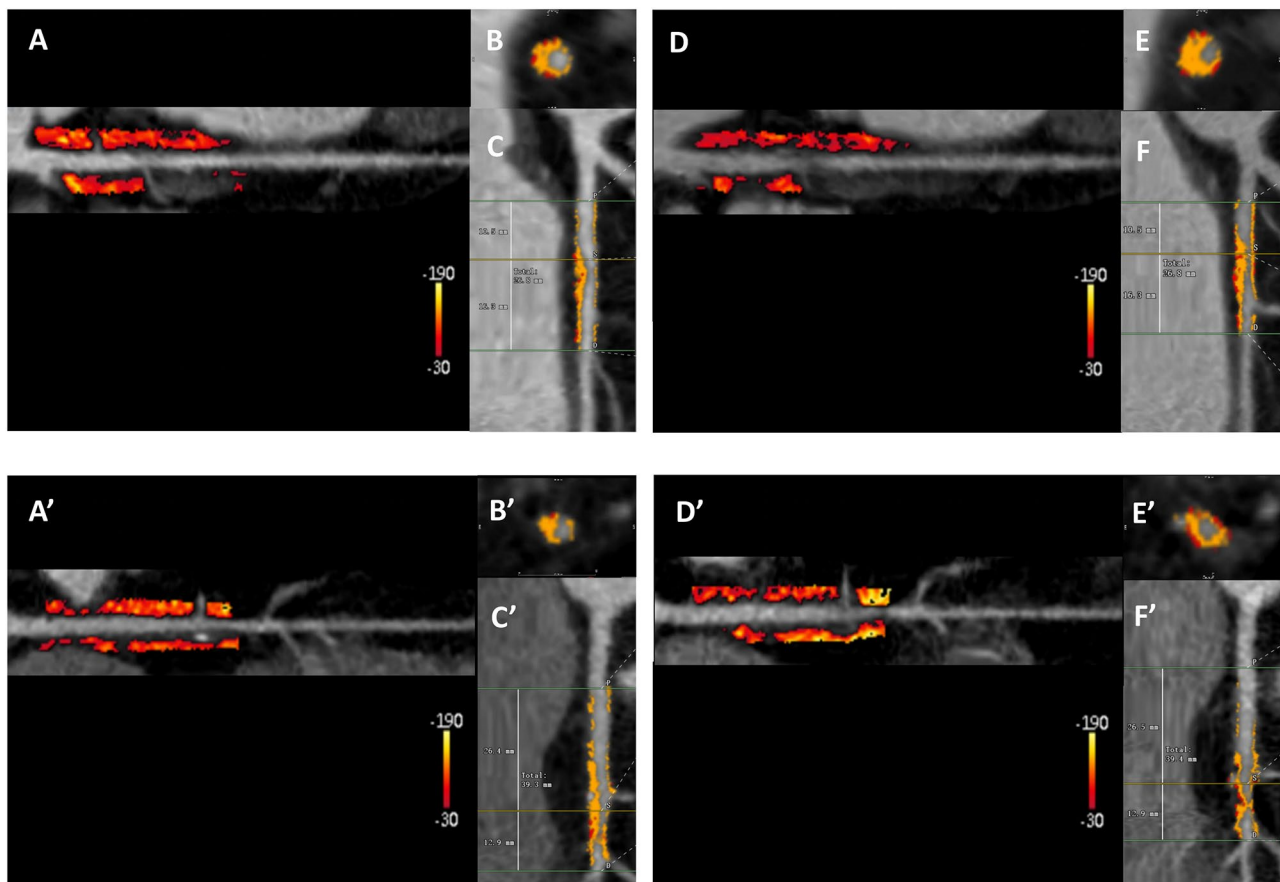


Fig. 2 Representative cases showing dynamic changes in plaque burden with pericoronary inflammation. Quantified PCAT attenuation and coronary PAV obtained from CCTA are presented. The straightened multiplanar view shows PCAT attenuation quantification, displayed using adipose tissue HU color mapping with corresponding color bars. Non-calcified, calcified, and low-attenuated plaques are represented by orange, yellow, and red overlays, respectively. **(A–F)** A representative plaque from the proximal left circumflex artery with increased PCAT attenuation and plaque progression. At baseline, overall, non-calcified, calcified, and low-attenuated PAV were 44.85%, 44.58%, 0.28%, and 4.38%, respectively. At follow-up, these values were 57.21%, 56.62%, 0.59%, and 7.23%. Baseline PCAT attenuation was -81 HU, and follow-up PCAT attenuation was -72 HU. **(A'–F')** A representative plaque from the proximal left anterior descending artery with decreased PCAT attenuation and plaque regression. At baseline, overall, non-calcified, calcified, and low-attenuated PAV were 47.02%, 46.93%, 0.08%, and 5.23%, respectively. At follow-up, these values were 30.29%, 30.29%, 0.00%, and 3.85%. Baseline PCAT attenuation was -82 HU, and follow-up PCAT attenuation was -89 HU. Abbreviations: CCTA, coronary computed tomographic angiography; HU, Hounsfield Unit; PAV, percent atheroma volume; PCAT, pericoronary adipose tissue

Table 1 Baseline characteristics of the study patients

	Total N= 89
Clinical characteristics	
Age, years	59.9±9.2
Male, n (%)	67 (75.3)
BMI, kg/m ²	25.5 (23.8, 29.0)
SBP, mmHg	127.9±15.9
DBP, mmHg	73.5±11.3
Risk factors, n (%)	
Hypertension	60 (67.4)
Dyslipidemia	74 (83.1)
Smoking	
Never	37 (41.6)
Former	23 (25.8)
Current	29 (32.6)
Medical histories, n (%)	
Myocardial infarction	8 (9.0)
Myocardial revascularization	27 (30.3)
Stroke	13 (14.6)
Serial CCTAs	
Time interval, month	13.5 (12.2, 17.5)
Baseline tube voltage, n (%)	
100 kV	61 (68.5)
120 kV	28 (31.5)
Number of study plaque, per patient	152 (1.71)
Medications, n (%)	
Aspirin	82 (92.1)
Statins	89 (100.0)
Ezetimibe	28 (31.5)
ACEI/ARB	42 (47.2)
Metformin	41 (46.1)
Incretins	16 (18.0)
DPP4i	13 (14.6)
GLP1ra	3 (3.4)
SGLT2i	45 (50.6)
Insulin	15 (16.9)

ACEI, angiotensin converting enzyme inhibitor; ARB, angiotensin II receptor blocker; BMI, body mass index; CCTA, coronary computed tomographic angiography; DBP, diastolic blood pressure; DPP4i, dipeptidyl peptidase-4 Inhibitors; GLP1ra, glucagon-like peptide-1 receptor agonists; SGLT2i, sodium-glucose cotransporter-2 inhibitor; SBP, systolic blood pressure

changes in overall and compositional PAV as dependent variables. Variables with a *p*-value < 0.1 in univariate analysis, as well as known accelerators of atherosclerotic plaque progression, were included in the multivariate model.

Given the variations in CCTA scan intervals, the independent association of δ PCAT attenuation with annualized δ PAV (changes in PAV divided by the number of years between CCTA scans) was calculated. Subgroup analyses were conducted to confirm whether the association between δ PCAT attenuation and changes in overall PAV remained consistent across pre-specified subgroups. Statistical significance was set at *p* < 0.05 (two-tailed). All statistical analyses were conducted using SPSS 25.0 (IBM Corporation, IL, USA) and R Programming Language 4.2.2 (Vienna, Austria).

Table 2 Changes of risk factors and CCTA findings of the study plaques

	Baseline (N= 152)	Follow-up (N= 152)	<i>p</i> value
Quantitative Risk Factors			
SBP, mmHg	128.3±15.34	125.6±12.4	0.075
DBP, mmHg	73.9±12.2	73.5±8.8	0.832
hs-CRP, mg/L	0.99 (0.60, 2.11)	0.66 (0.45, 1.02)	< 0.001
FPG, mmol/L	7.4 (5.9, 8.6)	6.9 (6.0, 7.8)	0.021
TG, mmol/L	1.48 (1.07, 2.21)	1.21 (0.84, 1.87)	< 0.001
TC, mmol/L	3.68 (3.17, 4.34)	3.30 (2.99, 3.69)	< 0.001
HDL-C, mmol/L	1.01 (0.85, 1.18)	1.06 (0.95, 1.27)	< 0.001
LDL-C, mmol/L	1.94 (1.50, 2.59)	1.42 (0.97, 1.67)	< 0.001
CCTA Findings			
Percent atheroma volume, %			
Overall	41.68±12.47	43.71±12.24	0.035
Calcified	1.85 (0.43, 6.32)	3.63 (0.77, 8.70)	< 0.001
Non-Calcified	37.01±13.59	36.97±13.51	0.966
Low-attenuated	5.54 (3.76, 9.06)	5.37 (3.46, 8.04)	0.068
Diameter stenosis, %	39.14±19.57	39.85±19.72	0.672

DBP, diastolic blood pressure; FPG, fasting plasma glucose; hs-CRP, hypersensitive C-reactive protein; HDL-C, high-density lipoprotein cholesterol; LDL-C, low-density lipoprotein cholesterol; SBP, systolic blood pressure; TG, triglyceride; TC, total cholesterol

Results

Characteristics of study patients and plaques at baseline and follow-up

A total of 175 patients with T2DM who underwent serial clinically indicated CCTA with a time interval of more than 12 months and the presence of more than one study plaque were initially screened. Finally, 89 eligible patients (mean age: 59.9 years; 75.3% men) with 152 study plaques were included. All patients had mCRFs meeting treatment targets at follow-up CCTA (Fig. 1; Table 1). Among the study population, hypertension (67.4%) and dyslipidemia (83.1%) were common, and approximately one-third had a history of myocardial revascularization at baseline. All patients were on statin therapy, approximately one-third were prescribed ezetimibe at discharge, and nearly half received sodium-glucose cotransporter-2 (SGLT-2) inhibitors.

Following a median of 13.5 months (IQR: 12.2, 17.5 months) of medical therapy, significant improvements were observed in FPG, lipid profiles, and hs-CRP levels (all *p* < 0.05), with a numerical reduction in BP (Table 2). However, CCTA plaque analysis revealed a significant increase in overall PAV [(41.68±12.47)% vs. (43.71±12.24)%], *p* = 0.035 (Table 2). Study plaques were further divided into those with overall PAV progression (δ PAV > 0, *n* = 80) and those without progression (δ PAV ≤ 0, *n* = 72). Compared to non-progressing plaques, those with progression demonstrated a significantly lower proportion of diameter stenosis ≥ 50% (18.8% vs. 36.1%, *p* = 0.016) but showed a markedly greater increase in PCAT attenuation from baseline [(5.9±9.2) HU vs. (1.4±7.7) HU], *p* = 0.002 (Table 3).

Table 3 Baseline characteristics according to overall plaque burden progression

	Progression (n = 80)	Non-progression (n = 72)	p value
Clinical characteristics			
Age, years	61.0 (53.3, 64.0)	62.0 (54.3, 67.0)	0.249
Male, n (%)	62 (77.5)	50 (69.4)	0.260
BMI, kg/m ²	25.3 (24.1, 29.4)	25.5 (24.0, 28.6)	0.561
SBP, mmHg	128.5 (118.0, 136.8)	131.5 (119.0, 139.5)	0.280
DBP, mmHg	76.0 (65.5, 81.0)	73.5 (65.0, 83.0)	0.940
Risk factors, n (%)			
Hypertension	56 (70.0)	48 (66.7)	0.659
Dyslipidemia	67 (83.8)	59 (81.9)	0.768
Smoking			0.843
Never	32 (40.0)	31 (43.1)	
Former	20 (25.0)	19 (26.4)	
Current	28 (35.0)	22 (30.6)	
Medical histories, n (%)			
Myocardial infarction	8 (10.0)	4 (5.6)	0.310
Myocardial revascularization	28 (35.0)	13 (18.1)	0.019
Stroke	17 (21.3)	10 (13.9)	0.236
Laboratory Findings			
FPG, mmol/L	8.1 ± 3.1	7.8 ± 3.2	0.605
Creatinine, μmol/L	74.0 (59.5, 86.4)	72.6 (66.1, 84.0)	0.903
TG, mmol/L	1.45 (1.03, 2.19)	1.60 (1.17, 2.41)	0.490
TC, mmol/L	3.60 (3.13, 4.29)	3.85 (3.23, 4.55)	0.180
HDL-C, mmol/L	1.00 (0.80, 1.11)	1.03 (0.89, 1.19)	0.155
LDL-C, mmol/L	1.84 (1.48, 2.12)	2.12 (1.51, 2.73)	0.072
hs-CRP, mg/L	0.84 (0.58, 1.82)	1.09 (0.64, 2.30)	0.098
Serial CCTAs			
Time interval, month	15.8 (12.8, 22.9)	14.2 (12.9, 23.3)	0.736
Baseline tube voltage, n (%)			0.254
100 kV	58 (72.5)	46 (63.9)	
120 kV	22 (27.5)	26 (36.1)	
Plaque location, n (%)			0.777
LAD	22 (27.5)	23 (31.9)	
LCX	31 (38.8)	28 (38.9)	
RCA	27 (33.8)	21 (29.2)	
Diameter stenosis ≥ 50%, n (%)	15 (18.8)	26 (36.1)	0.016
PCAT attenuation, HU			
Baseline	-81.9 ± 9.6	-81.1 ± 8.2	0.597
Follow-up	-76.1 ± 9.2	-79.7 ± 9.9	0.020
Change from baseline	5.9 ± 9.2	1.4 ± 7.7	0.002
Medications, n (%)			
Aspirin	74 (92.5)	64 (88.9)	0.442
Statins	80 (100.0)	72 (100.0)	1.000
Ezetimibe	24 (30.0)	23 (31.9)	0.796
ACEI/ARB	39 (48.8)	34 (47.2)	0.851
Metformin	42 (52.5)	30 (41.7)	0.182
Incretins	18 (22.5)	11 (15.3)	0.258
DPP4i	16 (20.0)	8 (11.1)	0.133
GLP1ra	2 (2.5)	3 (4.2)	0.905
SGLT2i	35 (43.8)	38 (52.8)	0.266
Insulin	12 (15.0)	15 (20.8)	0.347

LAD, left anterior descending artery; LCX, left circumflex coronary artery; PCAT, pericoronary adipose tissue; RCA, right coronary artery. Other abbreviations referring to Tables 1 and 2

Dynamic changes of compositional PAV with PCAT attenuation

Study plaques were divided into two subgroups based on pericoronary inflammation progression: δ PCAT attenuation >0 ($n=88$) and δ PCAT attenuation ≤ 0 ($n=64$). After a median follow-up of 13.5 months, plaques with δ PCAT attenuation >0 showed a significant increase in overall PAV [(39.24 \pm 12.87)% vs. (43.33 \pm 12.13)%, $p=0.002$] and calcified PAV [1.66% (IQR: 0.41, 6.29) vs. 3.73% (IQR: 1.05, 9.16), $p<0.001$] from baseline. Similarly, plaques with δ PCAT attenuation ≤ 0 also demonstrated a significant increase in calcified PAV [2.47% (IQR: 0.49, 6.80) vs. 3.56% (IQR: 0.58, 8.11), $p=0.003$] from baseline (Fig. 3, Table S1). Furthermore, compared to plaques with δ PCAT attenuation ≤ 0 , those with δ PCAT attenuation >0 had significantly greater changes in overall PAV [(4.09 \pm 12.09)% vs. (-0.82 \pm 10.74)%, $p=0.011$] and calcified PAV [1.57% (IQR: 0.13, 3.84) vs. 0.38% (IQR: -0.26, 2.58), $p=0.008$]. Additionally, plaques with δ PCAT attenuation >0 showed numerically higher changes in non-calcified PAV [(1.29 \pm 11.75)% vs. (-1.87 \pm 10.47)%, $p=0.089$] (Fig. 3, Table S1). The inter-observer variability for overall PAV was 0.92, while intra-observer variability was 0.94.

Association of changes in PCAT attenuation with compositional PAV

Correlation analysis revealed a positive relationship between δ PCAT attenuation and changes in overall PAV ($r=0.28$, $p=0.001$), calcified PAV ($r=0.27$, $p=0.001$), and non-calcified PAV ($r=0.22$, $p=0.007$), while no correlation was observed between δ PCAT attenuation and changes in low-attenuated PAV ($p>0.05$) (Fig. 4). This positive relationship between δ PCAT attenuation and changes in overall, calcified, and non-calcified PAV was also maintained in the univariable analysis (Table 4). Furthermore, three multivariate models were established to evaluate the relationship between δ PCAT attenuation and compositional plaque progression. In the fully adjusted multivariate model (model 3), which adjusted for age, sex, baseline and changes in risk factors, smoking status, medications, CCTA scan interval, scan parameters, and baseline compositional PAV and PCAT attenuation, δ PCAT attenuation was positively and independently associated with changes in overall PAV ($\beta=0.339$, $p=0.002$), changes in calcified PAV ($\beta=0.109$, $p=0.018$), and changes in non-calcified PAV ($\beta=0.237$, $p=0.034$) (Table 4).

The relationship between δ PCAT attenuation and changes in compositional PAV was further validated

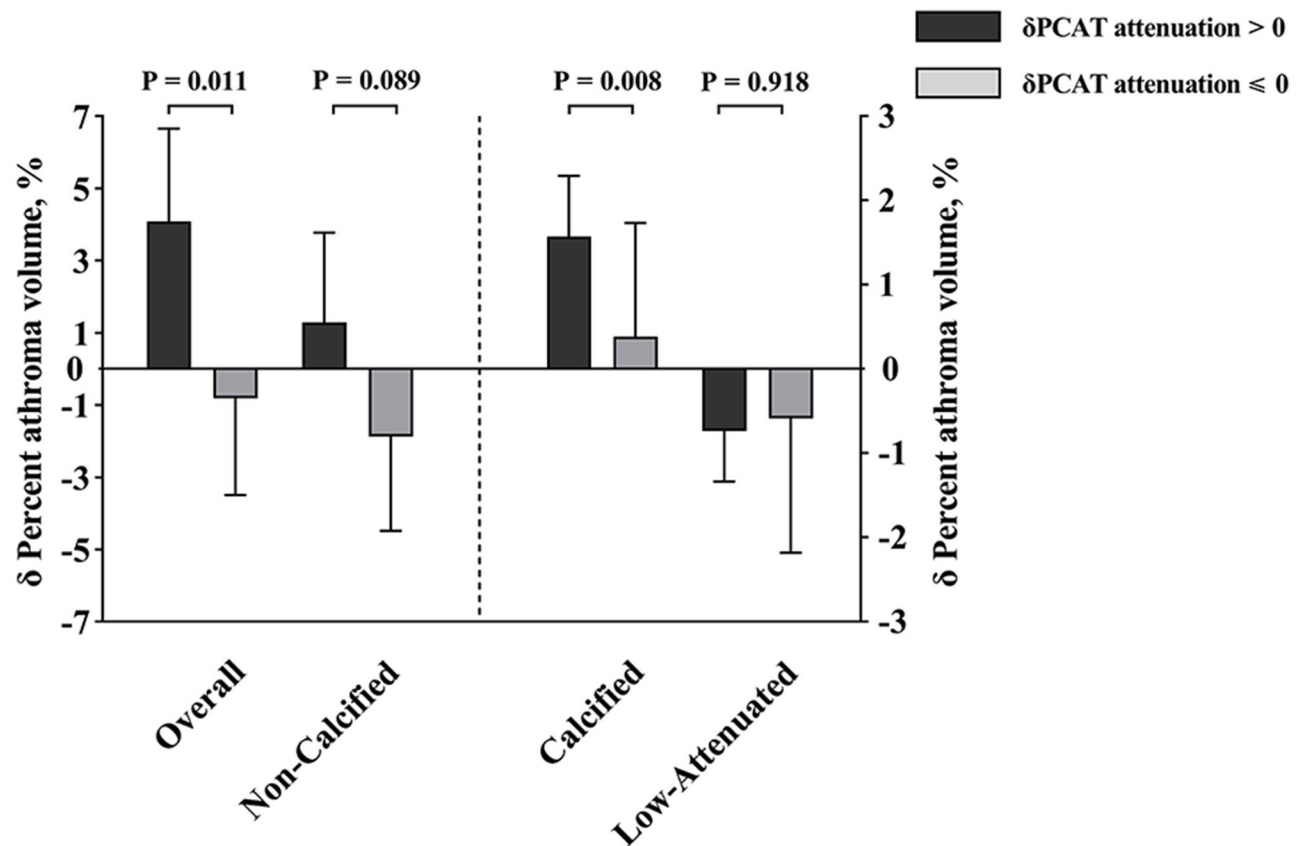


Fig. 3 Changes in plaque burden according to increased or decreased pericoronary inflammation. Abbreviation: PCAT, pericoronary adipose tissue

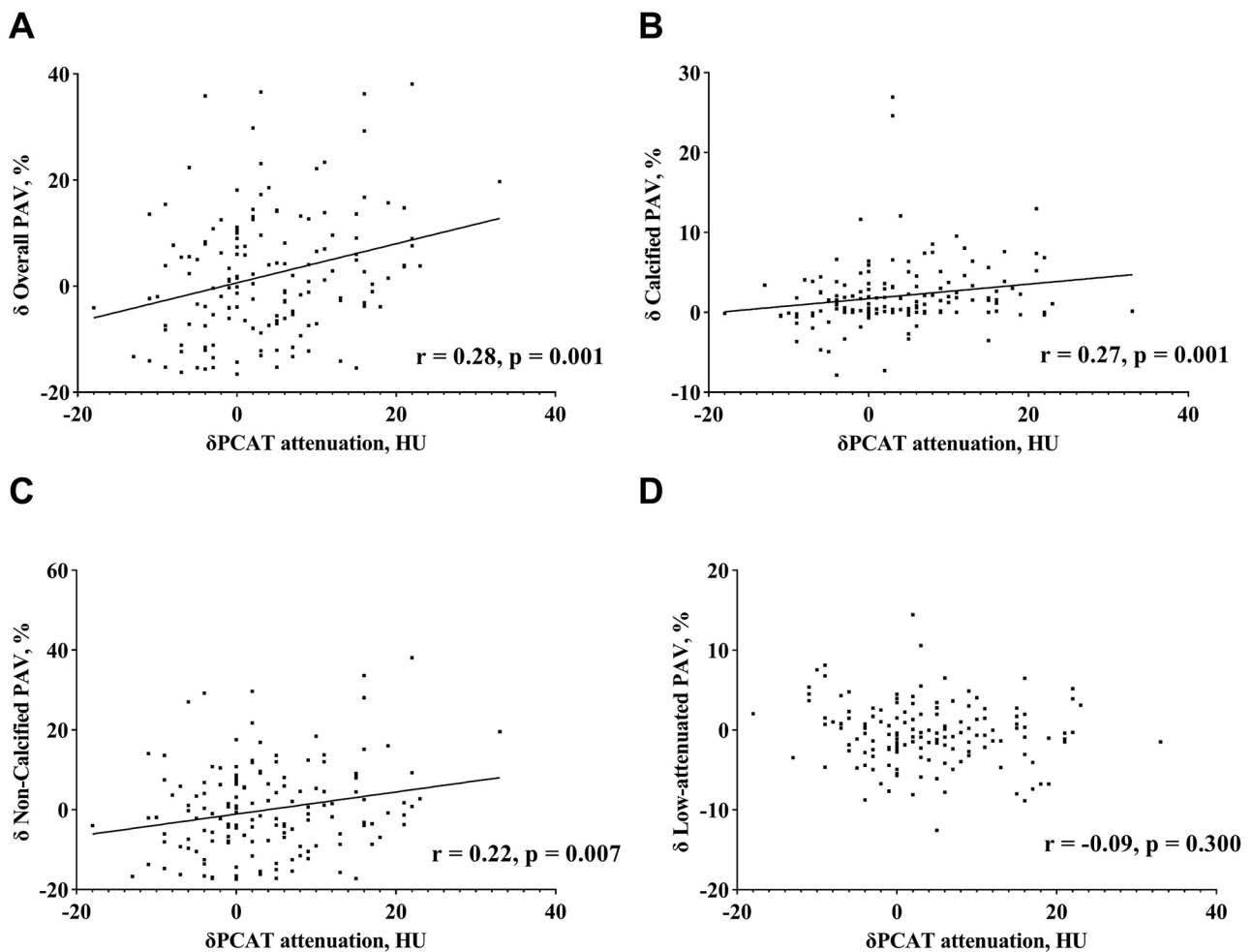


Fig. 4 Correlation analysis between changes in pericoronary inflammation and changes in plaque burden. Abbreviations: HU, Hounsfield Unit; PAV, percent atheroma volume; PCAT, pericoronary adipose tissue

in a sensitivity analysis, where δ PCAT attenuation was divided by annual δ PAV to account for variations in CCTA scan intervals among study plaques (Table S2).

Subgroup analysis

Subgroup analysis was conducted to assess whether the association between elevated PCAT attenuation and overall PAV progression was consistent across pre-specified subgroups. These subgroups included age (<65 years or ≥ 65 years), sex (male or female), body mass index ($BMI < 24$ or ≥ 24 kg/m²), hypertension (presence or absence), smoking status (current, former, or never), hs-CRP levels (<1.00 or ≥ 1.00 mmol/L), LDL-C (<1.94 or ≥ 1.94 mmol/L), and FPG (<7.4 or ≥ 7.4 mmol/L). After adjusting for medications, baseline PCAT attenuation, overall PAV, time interval, and tube voltage, no significant interactions were identified between δ PCAT attenuation and changes in overall PAV progression across any of the subgroups (p for interaction > 0.05) (Fig. 5).

Discussion

In this longitudinal cohort of patients with T2DM who achieved improved mCRFs, the main findings were as follows: Despite significant improvements in BP, LDL-C, FPG, and hs-CRP after optimal medical therapy over a median follow-up period of 13.5 months, PAV increased from baseline in more than half of the study plaques. The progression of coronary inflammation, quantified by PCAT attenuation, was positively and independently associated with the progression of overall PAV, primarily driven by non-calcified PAV. This association persisted after adjusting for age, sex, cardiovascular risk factors, concurrent medications, CCTA scan intervals and parameters, as well as baseline PAV and PCAT attenuation.

Residual cardiovascular risk and inflammation evaluation

Lipid-lowering therapy, particularly targeting LDL-C, has traditionally been the cornerstone of preventing the progression of atherosclerosis and subsequent cardiovascular

Table 4 Associations of changes of pericoronary inflammation with progression of plaque burden

	Model*	Continuous Plaque Progression	
		β † (95%CI)	p value
Compositional PAV			
Overall	Univariable	0.368 (0.161, 0.575)	0.001
	Model 1	0.364 (0.156, 0.571)	0.001
	Model 2	0.372 (0.164, 0.579)	0.001
	Model 3	0.339 (0.129, 0.549)	0.002
Calcified	Univariable	0.091 (0.015, 0.166)	0.019
	Model 1	0.118 (0.029, 0.206)	0.010
	Model 2	0.108 (0.019, 0.197)	0.018
	Model 3	0.109 (0.019, 0.200)	0.018
Non-Calcified	Univariable	0.277 (0.075, 0.479)	0.007
	Model 1	0.268 (0.050, 0.485)	0.016
	Model 2	0.280 (0.064, 0.496)	0.011
	Model 3	0.237 (0.019, 0.455)	0.034
Low-attenuated	Univariable	-0.050 (-0.121, 0.021)	0.166
	Model 1	-0.039 (-0.108, 0.030)	0.270
	Model 2	-0.033 (-0.102, 0.036)	0.347
	Model 3	-0.046 (-0.116, 0.023)	0.189

FAI, fat attenuation index; PAV, percent atheroma volume

*Variables in model 1 consisted of age, sex, BMI, SBP, FPG, LDL-C, hs-CRP, PCAT attenuation, smoking status, aspirin, insulin, SGLT2i, time interval, tube voltage, baseline compositional PAV and δ PCAT attenuation

Variables in model 2 consisted of age, sex, BMI, δ SBP, δ FPG, δ LDL-C, δ hs-CRP, PCAT attenuation, smoking status, aspirin, insulin, SGLT2i, time interval, tube voltage, baseline compositional PAV and δ PCAT attenuation

Variables in model 3 consisted of age, sex, BMI, SBP, FPG, LDL-C, hs-CRP, PCAT attenuation, smoking status, δ SBP, δ FPG, δ LDL-C, δ hs-CRP, aspirin, insulin, SGLT2i, time interval, tube voltage, baseline compositional PAV and δ PCAT attenuation

† The β value was examined by per 1HU increase of δ PCAT attenuation

events [18]. However, even in patients achieving LDL-C targets, atherosclerotic plaques may continue to progress, contributing to cardiovascular events. In the present study, despite significant improvements in LDL-C, BP, FPG, and hs-CRP, an increase in overall PAV was observed in 52.6% of study plaques. This underscores the need for addressing residual cardiovascular risk beyond traditional modifiable factors, with inflammation emerging as a key therapeutic target [19].

A recent meta-analysis involving 175,778 individuals demonstrated that PCAT attenuation assessed using routine CCTA images was a superior prognostic biomarker compared to circulating hs-CRP levels [20]. Although PCAT volume is also considered a potential marker of inflammation [21, 22], PCAT attenuation has been biologically and clinically validated as a more reliable indicator of pericoronary inflammation [10, 23]. This distinction was evident in our study, where approximately 58% of study plaques showed elevated vascular inflammation (δ PCAT attenuation > 0), even among patients with improved mCRFs, including hs-CRP levels below 2 mg/L.

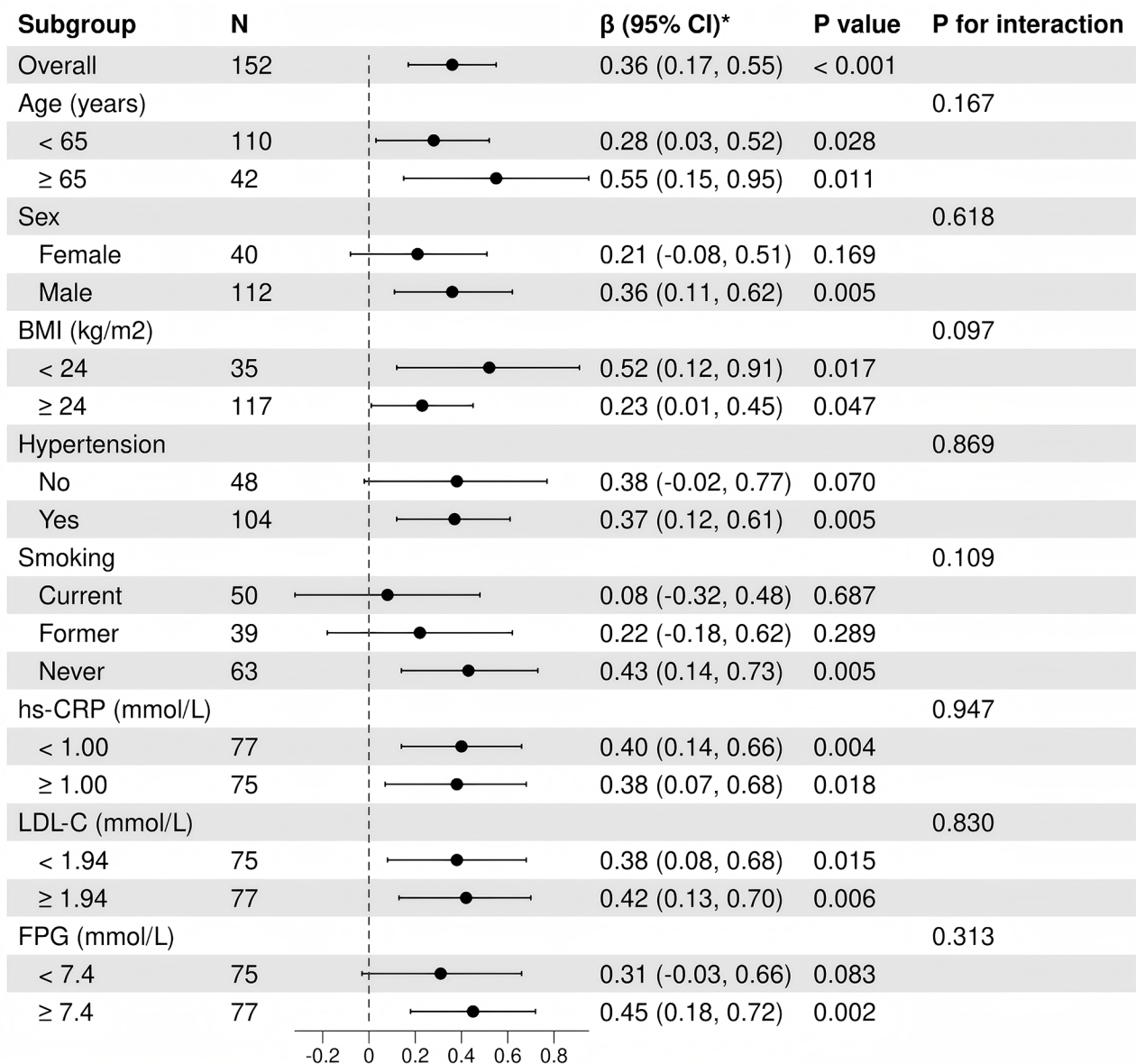
Diabetes accelerated atherosclerotic plaque

Increased atherosclerotic plaque burden, quantified as PAV, is a validated imaging surrogate for predicting future adverse cardiovascular events [24]. In the Progression of Atherosclerotic Plaque Determined by Computed Tomographic Angiography Imaging (PARADIGM) registry, which included 1,296 subjects, Won et al. demonstrated that diabetes had an incremental effect on PAV progression (odds ratio [OR]: 1.64, $p=0.01$) over a median follow-up of 3.2 years [25]. In a subgroup analysis of 402 patients without coronary plaques at baseline within the same registry, glycemic control was found to be independently associated with the annual change in PAV ($\beta=0.10$, $p<0.001$) [26]. Furthermore, Won et al. reported that the triglyceride glucose index, a reliable marker of insulin resistance, was significantly associated with rapid PAV progression (OR: 1.78, $p<0.001$) [27]. This series of studies highlights the significant role of diabetes and glycemic control in PAV progression, offering a partial explanation for the approximately two- to four-fold higher risk of adverse cardiac events in individuals with diabetes compared to non-diabetic subjects [28]. Importantly, novel antidiabetic therapies, including sodium-glucose cotransporter-2 inhibitors and glucagon-like peptide-1 receptor agonists, have demonstrated cardiovascular outcome benefits, likely due to their effects on delaying plaque progression [19, 29].

Coronary inflammation accelerated atherosclerotic plaque

Elevated PCAT attenuation has been shown to be significantly associated with the burden of non-calcified plaque as opposed to calcified plaque [30], and the presence of vulnerable plaque components [31]. To further investigate the relationship between PCAT attenuation and atherosclerotic plaque progression, Lee et al. conducted an exploratory analysis of the PARADIGM registry. In a low-risk CAD population comprising 474 patients and 1,476 lesions with a mean diameter stenosis of $18.8\% \pm 12.6\%$, they observed that increased PCAT attenuation was positively correlated with total plaque volume progression ($\beta=0.275$, $p=0.047$), primarily driven by fibrous plaque volume ($\beta=0.245$, $p=0.006$). However, their study had significant limitations, including insufficient adjustment for residual cardiovascular risk factors, such as baseline PCAT attenuation, baseline hs-CRP, and dynamic changes in mCRFs (e.g., δ systolic blood pressure [δ SBP], δ FPG, and δ hs-CRP [23]).

To address these limitations, our study enrolled patients with T2DM, a high-risk population characterized by increased coronary inflammation and complex plaque features, who achieved improved mCRFs. In this population, we confirmed the independent association between δ PCAT attenuation and progression of overall PAV, particularly non-calcified PAV. These findings were



* adjusted for Aspirin, Insulin, Incretins, SGLT2i, baseline PCAT attenuation, overall PAV, time interval and tube voltage

Fig. 5 Subgroup analysis for the impact of changes in pericoronary inflammation on changes of overall plaque burden. The black vertical dotted line represents a β value of 0. The subgroup analysis was adjusted for medications, baseline PCAT attenuation, overall PAV, time interval, and tube voltage. Abbreviations: BMI, body mass index; FPG, fasting plasma glucose; hs-CRP, high-sensitivity C-reactive protein; LDL-C, low-density lipoprotein cholesterol; PAV, percent atheroma volume; PCAT, pericoronary adipose tissue; SGLT2i, sodium-glucose cotransporter-2 inhibitor

consistent in the sensitivity analyses, subgroup analyses, and multivariate models, which accounted for baseline PCAT attenuation, baseline hs-CRP, and dynamic changes in key mCRFs (e.g., δ SBP, δ FPG, δ LDL-C, and δ hs-CRP).

Interestingly, we did not observe a significant correlation between δ PCAT attenuation and changes in low-attenuated PAV, which may be attributed to the use of moderate-intensity statins and improved mCRFs, both of

which could attenuate low-attenuated plaques. Additionally, unlike the findings by Goeller et al. [32] and Lee et al. [23], our study revealed a positive correlation between δ PCAT attenuation and changes in calcified PAV. This discrepancy may be explained by our study population, which consisted of diabetic patients receiving the treatment of statins, both of which are known contributors to vascular calcification [19, 20, 23].

Clinical implication

The integration of PCAT attenuation as a non-invasive imaging biomarker allows clinicians to dynamically assess residual cardiovascular risk beyond traditional markers, such as LDL-C and hs-CRP. This approach is particularly important for patients with CAD who are at increased risk for future cardiovascular events, including those with T2DM, a history of myocardial infarction, or prior coronary revascularization, regardless of their traditional risk factors. Routine CCTA with serial evaluation of PCAT attenuation offers a novel strategy to enhance risk stratification in CAD. Additionally, PCAT attenuation may be valuable for developing novel treatments targeting vascular inflammation and for monitoring the efficacy of treatments over time.

Study limitations

This study had several limitations. Firstly, it was a single-center, retrospective study with a relatively small sample size. The initial cohort consisted of high-risk T2DM patients, with or without prior revascularization. In real-world practice, such patients would typically undergo invasive angiography rather than repeat CCTA if they presented with new symptoms, which may limit the generalizability of our findings. Meanwhile, a direct causal relationship between increased pericoronary inflammation and plaque progression could not be established. However, this study uniquely examined a real-world diabetic cohort with well-controlled risk factors, highlighting that the progression of coronary plaques may be attributed to increased coronary inflammation and emphasizing the need to address residual perivascular inflammation. Secondly, the study population had varied risk profiles and treatment targets for mCRFs, yet a broad and uniform criterion (e.g., BP target < 140/90 mmHg) was applied to all patients. Thirdly, control of mCRFs was assessed only at baseline and at the time of the last CCTA examination, making it impossible to evaluate dynamic changes in these factors between consecutive CCTA examinations. Additionally, certain important data, such as hemoglobin A1c levels and detailed information on medical treatments during follow-up, were unavailable due to the retrospective design of the study.

Conclusion

In this longitudinal CCTA cohort of T2DM patients with improved management of mCRFs, increased PCAT attenuation, measured from routine CCTA, was associated with the progression of overall PAV, particularly non-calcified PAV. These findings highlighted a potential link between perivascular inflammation and atherosclerotic plaque progression, suggesting that PCAT attenuation could serve as a promising imaging biomarker for monitoring plaque progression in the diabetic population.

Abbreviations

CAD	Coronary Artery Disease
CCTA	Coronary Computed Tomography Angiography
FPG	Fasting Plasma Glucose
hs-CRP	High-Sensitivity C-Reactive Protein
HU	Hounsfield Unit
IQR	Interquartile Range
LDL-C	Low-Density Lipoprotein Cholesterol
mCRFs	Modifiable Cardiovascular Risk Factors
PAV	Percent Atheroma Volume
PCAT	Pericoronary Adipose Tissue
PARADIGM	Progression of Atherosclerotic Plaque Determined by Computed Tomographic Angiography Imaging
T2DM	Type 2 Diabetes Mellitus

Supplementary Information

The online version contains supplementary material available at <https://doi.org/10.1186/s13098-025-01645-4>.

Supplementary Material 1

Acknowledgements

None.

Author contributions

THZ, XLG, TLC, HKZ, XMZ, JYY, YZ, YLP, and XNM were involved in data collection and analysis; THZ, PAP, YD, ZJW and DMS were responsible for drafting the manuscript; LX, YJZ, and YD contributed to the study design and provided intellectual guidance. All the authors have read and approved the final manuscript for publication.

Funding

This work was supported by the grant from Noncommunicable Chronic Diseases-National Science and Technology Major Project (2023ZD0514900), National Key Research and Development Program of China (2022YFC3602500); National Key Research and Development Program of China (2023ZD0514900); and Beijing Natural Science Foundation (7244326).

Data availability

The datasets used/or analyzed during the current study are available from the corresponding author on reasonable request.

Declarations

Ethics approval and consent to participate

This research protocol was approved by the Clinical Research Ethics Committee of Beijing Anzhen Hospital, Capital Medical University, with informed consent obtained from all study participants.

Consent for publication

If the manuscript is accepted, we approve it for publication in *Diabetology & Metabolic Syndrome*.

Competing interests

The authors declare no competing interests.

Author details

¹Department of Cardiology, Beijing Anzhen Hospital, Capital Medical University, Beijing 100029, China

²Department of Radiology, Beijing Anzhen Hospital, Capital Medical University, Beijing 100029, China

³Beijing Institute of Heart Lung and Blood Vessel Disease, Beijing 100029, China

⁴Department of Radiology, Beijing Anzhen Nanchong Hospital of Capital Medical University & Nanchong Central Hospital, Nanchong 637000, China

Received: 23 December 2024 / Accepted: 18 February 2025

Published online: 25 February 2025

References

1. Knuuti J, Wijns W, Saraste A, Capodanno D, Barbato E, Funck-Brentano C, Prescott E, Storey RF, Deaton C, Cuisset T, et al. 2019 ESC guidelines for the diagnosis and management of chronic coronary syndromes. *EUR HEART J*. 2020;41(3):407–77.
2. Virani SS, Newby LK, Arnold SV, Bittner V, Brewer LC, Demeter SH, Dixon DL, Fearon WF, Hess B, Johnson HM, et al. 2023 AHA/ACC/ACCP/ASPC/NLA/PCNA guideline for the management of patients with chronic coronary disease: A report of the American heart association/american college of cardiology joint committee on clinical practice guidelines. *J AM COLL CARDIOL*. 2023;82(9):833–955.
3. Ginsberg HN, Packard CJ, Chapman MJ, Boren J, Aguilar-Salinas CA, Avena M, Ference BA, Gaudet D, Hegele RA, Kersten S, et al. Triglyceride-rich lipoproteins and their remnants: metabolic insights, role in atherosclerotic cardiovascular disease, and emerging therapeutic strategies—a consensus statement from the European atherosclerosis society. *EUR HEART J*. 2021;42(47):4791–806.
4. Gomez-Delgado F, Raya-Cruz M, Katsiki N, Delgado-Lista J, Perez-Martinez P. Residual cardiovascular risk: when should we treat it? *EUR J INTERN MED*. 2024;120:17–24.
5. Yuki H, Sugiyama T, Suzuki K, Kinoshita D, Niida T, Nakajima A, Araki M, Dey D, Lee H, McNulty I, et al. Coronary inflammation and plaque vulnerability: A coronary computed tomography and optical coherence tomography study. *CIRC-CARDIOVASC IMAG*. 2023;16(3):e014959.
6. O MK, ^ KM, İ SK, Düz Y, AŞ R. The relationship between mortality and Leuko-Glycemic index in coronary care unit patients (MORCOR-TURK LGI). *Dicle Tip Dergisi*. 2024;3(51):315–24.
7. Ridker PM, Bhatt DL, Pradhan AD, Glynn RJ, MacFadyen JG, Nissen SE. Inflammation and cholesterol as predictors of cardiovascular events among patients receiving Statin therapy: a collaborative analysis of three randomised trials. *Lancet*. 2023;401(10384):1293–301.
8. Ridker PM, Everett BM, Thuren T, MacFadyen JG, Chang WH, Ballantyne C, Fonseca F, Nicolau J, Koenig W, Anker SD, et al. Antiinflammatory therapy with Canakinumab for atherosclerotic disease. *NEW ENGL J MED*. 2017;377(12):1119–31.
9. Punnanithinont N, Kambalapalli S, Iskander B, Ichikawa K, Krishnan S, Lakshmanan S, Roy SK, Budoff M. Anti-inflammatory therapies in Atherosclerosis - Where are we going? *CURR ATHEROSCLER REP*. 2024;27(1):19.
10. Antoniadou C, Tousoulis D, Vavlukis M, Fleming I, Duncker DJ, Eringa E, Manfredini O, Antonopoulos AS, Oikonomou E, Padro T, et al. Perivascular adipose tissue as a source of therapeutic targets and clinical biomarkers. *EUR HEART J*. 2023;44(38):3827–44.
11. Antonopoulos AS, Angelopoulos A, Papanikolaou P, Simantiris S, Oikonomou EK, Vamvakaris K, Koumpoura A, Farmaki M, Trivella M, Vlachopoulos C, et al. Biomarkers of vascular inflammation for cardiovascular risk prognostication: A Meta-Analysis. *JACC-CARDIOVASC IMAG*. 2022;15(3):460–71.
12. Liu Y, Dai L, Dong Y, Ma C, Cheng P, Jiang C, Liao H, Li Y, Wang X, Xu X. Coronary inflammation based on pericoronary adipose tissue Attenuation in type 2 diabetic mellitus: effect of diabetes management. *CARDIOVASC DIABETOL*. 2024;23(1):108.
13. Abbara S, Blanke P, Maroules CD, Cheezum M, Choi AD, Han BK, Marwan M, Naoum C, Norgaard BL, Rubinshtein R, et al. SCCT guidelines for the performance and acquisition of coronary computed tomographic angiography: A report of the society of cardiovascular computed tomography guidelines committee: endorsed by the North American society for cardiovascular imaging (NASCI). *J CARDIOVASC COMPUT*. 2016;10(6):435–49.
14. Shaw LJ, Blankstein R, Bax JJ, Ferencik M, Bittencourt MS, Min JK, Berman DS, Leipsic J, Villines TC, Dey D, et al. Society of cardiovascular computed Tomography / North American society of cardiovascular imaging - Expert consensus document on coronary CT imaging of atherosclerotic plaque. *J CARDIOVASC COMPUT*. 2021;15(2):93–109.
15. Sheahan M, Ma X, Paik D, Obuchowski NA, St PS, Newman WR, Rae G, Perlman ES, Rosol M, Keith JJ, et al. Atherosclerotic plaque tissue: noninvasive quantitative assessment of characteristics with Software-aided measurements from conventional CT angiography. *Radiology*. 2018;286(2):622–31.
16. Dey D, Schepis T, Marwan M, Slomka PJ, Berman DS, Achenbach S. Automated three-dimensional quantification of noncalcified coronary plaque from coronary CT angiography: comparison with intravascular US. *Radiology*. 2010;257(2):516–22.
17. Antonopoulos AS, Sanna F, Sabharwal N, Thomas S, Oikonomou EK, Herdman L, Margaritis M, Shirodaria C, Kampoli AM, Akoumianakis I et al. Detecting human coronary inflammation by imaging perivascular fat. *SCI TRANSL MED* 2017, 9(398).
18. Dai X, Yu L, Lu Z, Shen C, Tao X, Zhang J. Serial change of perivascular fat Attenuation index after Statin treatment: insights from a coronary CT angiography follow-up study. *INT J CARDIOL*. 2020;319:144–9.
19. Zhang T, Gao X, Chen T, Zhang H, Zhang X, Xin Y, Shi D, Du Y, Xu L, Zhou Y. Longitudinal assessment of coronary plaque regression related to sodium-glucose cotransporter-2 inhibitor using coronary computed tomography angiography. *CARDIOVASC DIABETOL*. 2024;23(1):267.
20. Lee SE, Chang HJ, Sung JM, Park HB, Heo R, Rizvi A, Lin FY, Kumar A, Hadamitzky M, Kim YJ, et al. Effects of Statins on coronary atherosclerotic plaques: the PARADIGM study. *JACC-CARDIOVASC IMAG*. 2018;11(10):1475–84.
21. Nogajski L, Mazuruk M, Kacperska M, Kurpias M, Maczewski M, Nowakowski M, Maczewski M, Michalowska I, Leszek P, Paterek A. Epicardial fat density obtained with computed tomography imaging - more important than volume? *CARDIOVASC DIABETOL*. 2024;23(1):389.
22. Uygur B, Celik O, Demir AR, Karakayali M, Arslan C, Otcu TH, Alis D, Yildirim C, Corekcioglu B, Erturk M. Epicardial adipose tissue volume predicts long term major adverse cardiovascular events in patients with type 2 diabetes. *TURK KARDIYOL DERN A*. 2021;49(2):127–34.
23. Lee SE, Sung JM, Andreini D, Al-Mallah MH, Budoff MJ, Cademartiri F, Chinnaiyan K, Choi JH, Chun EJ, Conte E, et al. Association between changes in perivascular adipose tissue density and plaque progression. *JACC-CARDIOVASC IMAG*. 2022;15(10):1760–7.
24. Iatan I, Guan M, Humphries KH, Yeoh E, Mancini G. Atherosclerotic coronary plaque regression and risk of adverse cardiovascular events: A systematic review and updated Meta-Regression analysis. *JAMA CARDIOL*. 2023;8(10):937–45.
25. Won KB, Lee SE, Lee BK, Park HB, Heo R, Rizvi A, Lin FY, Kumar A, Hadamitzky M, Kim YJ, et al. Longitudinal assessment of coronary plaque volume change related to glycemic status using serial coronary computed tomography angiography: A PARADIGM (Progression of atherosclerotic plaque determined by computed tomographic angiography Imaging) substudy. *J CARDIOVASC COMPUT*. 2019;13(2):142–7.
26. Won KB, Lee BK, Lin FY, Hadamitzky M, Kim YJ, Sung JM, Conte E, Andreini D, Pontone G, Budoff MJ, et al. Glycemic control is independently associated with rapid progression of coronary atherosclerosis in the absence of a baseline coronary plaque burden: a retrospective case-control study from the PARADIGM registry. *CARDIOVASC DIABETOL*. 2022;21(1):239.
27. Won KB, Lee BK, Park HB, Heo R, Lee SE, Rizvi A, Lin FY, Kumar A, Hadamitzky M, Kim YJ, et al. Quantitative assessment of coronary plaque volume change related to triglyceride glucose index: the progression of atherosclerotic plaque determined by computed tomographic angiography imaging (PARADIGM) registry. *CARDIOVASC DIABETOL*. 2020;19(1):113.
28. Gregg EW, Sattar N, Ali MK. The changing face of diabetes complications. *LANCET DIABETES ENDO*. 2016;4(6):537–47.
29. Wong ND, Sattar N. Cardiovascular risk in diabetes mellitus: epidemiology, assessment and prevention. *NAT REV CARDIOL*. 2023;20(10):685–95.
30. Ma R, van Assen M, Ties D, Pelgrim GJ, van Dijk R, Sidorenkov G, van Ooijen P, van der Harst P, Vliegenthart R. Focal pericoronary adipose tissue Attenuation is related to plaque presence, plaque type, and stenosis severity in coronary CTA. *EUR RADIOLOG*. 2021;31(10):7251–61.
31. Sun JT, Sheng XC, Feng Q, Yin Y, Li Z, Ding S, Pu J. Pericoronary fat Attenuation index is associated with vulnerable plaque components and local Immune-Inflammatory activation in patients with Non-ST elevation acute coronary syndrome. *J AM HEART ASSOC*. 2022;11(2):e022879.
32. Goeller M, Tamarappoo BK, Kwan AC, Cadet S, Commandeur F, Razipour A, Slomka PJ, Gransar H, Chen X, Otaki Y, et al. Relationship between changes in pericoronary adipose tissue Attenuation and coronary plaque burden quantified from coronary computed tomography angiography. *EUR HEART J-CARD IMG*. 2019;20(6):636–43.

Publisher's note

Springer Nature remains neutral with regard to jurisdictional claims in published maps and institutional affiliations.